Supporting Information

Robust, multiscale liquid-metal patterning enabled by a sacrificial sealing layer for flexible and wearable wireless powering

Long Teng, Lifei Zhu, Stephan Handschuh-Wang, and Xuechang Zhou*

College of Chemistry and Environmental Engineering,
Shenzhen University, Shenzhen, 518060, P. R. China
Fax: (+) 86-755-26536141; Tel: (+) 86-755-26536627
E-mail: xczhou@szu.edu.cn (X. C. Z.)

Guangdong Laboratory of Artificial Intelligence and Digital Economy (SZ), Shenzhen University,
Shenzhen 518060, P. R. China

Movie 1: Removal of the adhesive tape by immersing in a water bath.

Movie 2: Removal of the PVA thin film by immersing in a water bach.

Movie 3: The charging of the battery of a cell phone by planar LM wireless power transmit coil.

Movie 4: The charging of the batter of a cell phone by bent LM wireless power transmit coil.

Movie 5: The powering of an LED light with a wearable LM wireless power transmission glove.

Movie 6: The powering of an electric fan with a wearable LM wireless power transmission glove

Movie 7: The powering of a wearable Bluetooth headset by flexible LM wireless transmit coil.

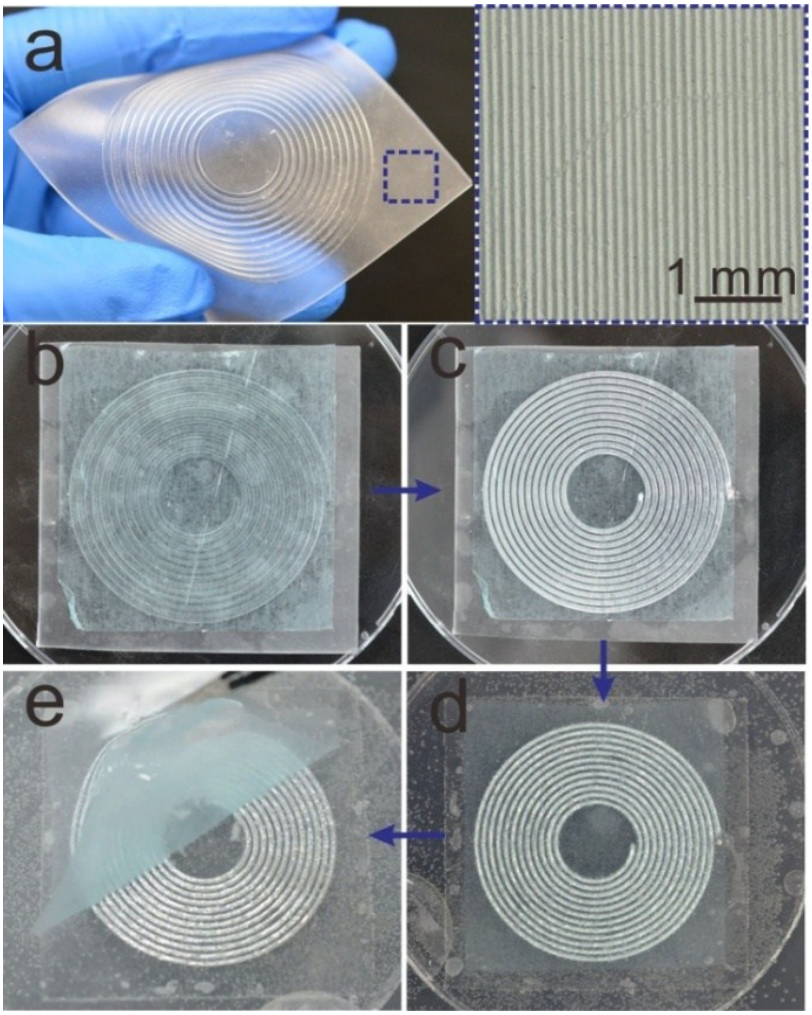

Figure S1. The fabrication process of an LM pattern enabled by the transiently sealing and subsequently dissolving of an adhesive tape. a) Digital (left) and optical microscopic (right) image of PDMS channels. b-e) Digital images of the process of LM patterning. b-c) A water-soluble acrylic tape is utilized to cover the channels of the PDMS substrate, followed by filling with LM. d) The LM-filled channel is then placed in DI water, where the glue of the acrylic tape is dissolved. e) The residue of the acrylic tape is removed in water smoothly and the LM pattern is obtained by drying in an oven.

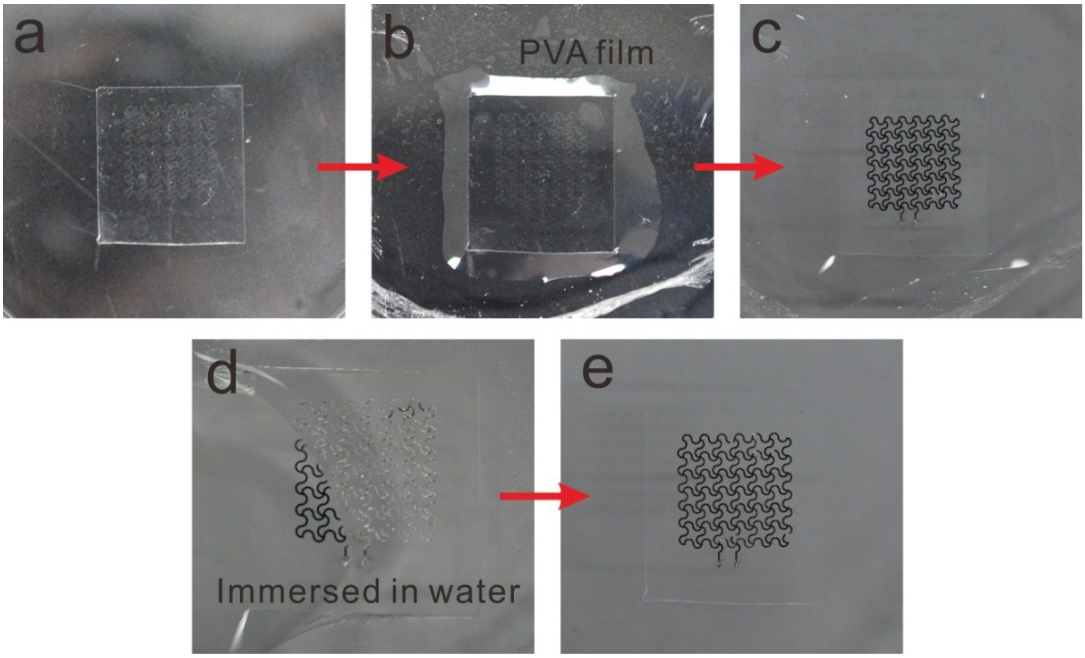

Figure S2. The fabrication process of an LM pattern enabled by the transiently sealing and subsequently dissolving of a PVA film. a-e) Digital images showing the process of LM patterning. a) The original PDMS microchannel. b-c) A PVA film was utilized to cover the channels of the PDMS substrate (b), followed by filling with LM (c). d) The LM-filled channel was then immersed in DI water, and the PVA film was dissolved. e) The LM pattern was obtained by drying in an oven.

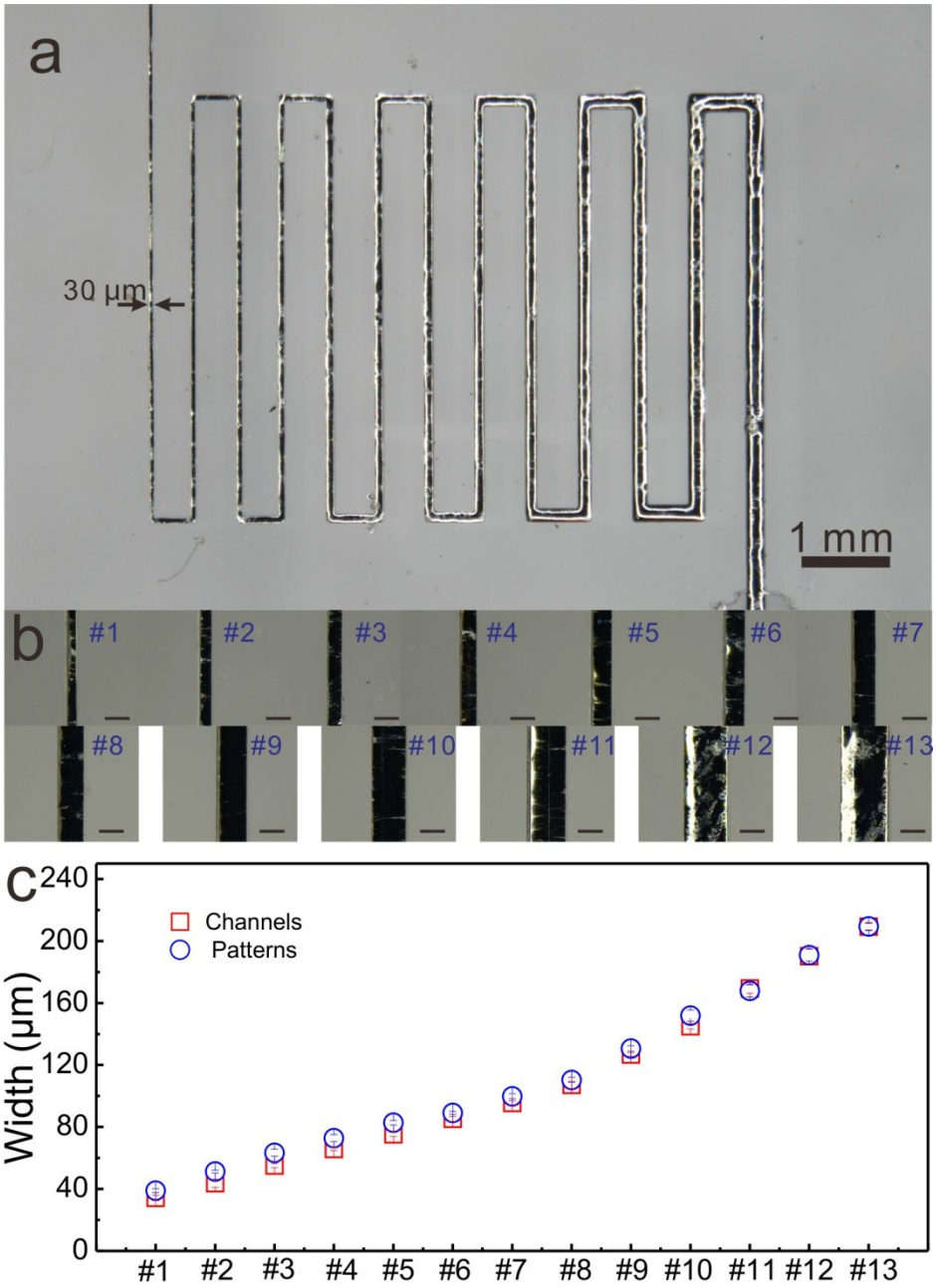

Figure S3. a) Microscopic image of an LM pattern prepared on PDMS with line width from 30 µm to 200 µm. b) Magnified images of patterns with different widths (#1–#13). (The scale bar is 100µm) c) Comparison of the width of the liquid metal patterns and the original microchannels. The experiment was repeated 3 times.

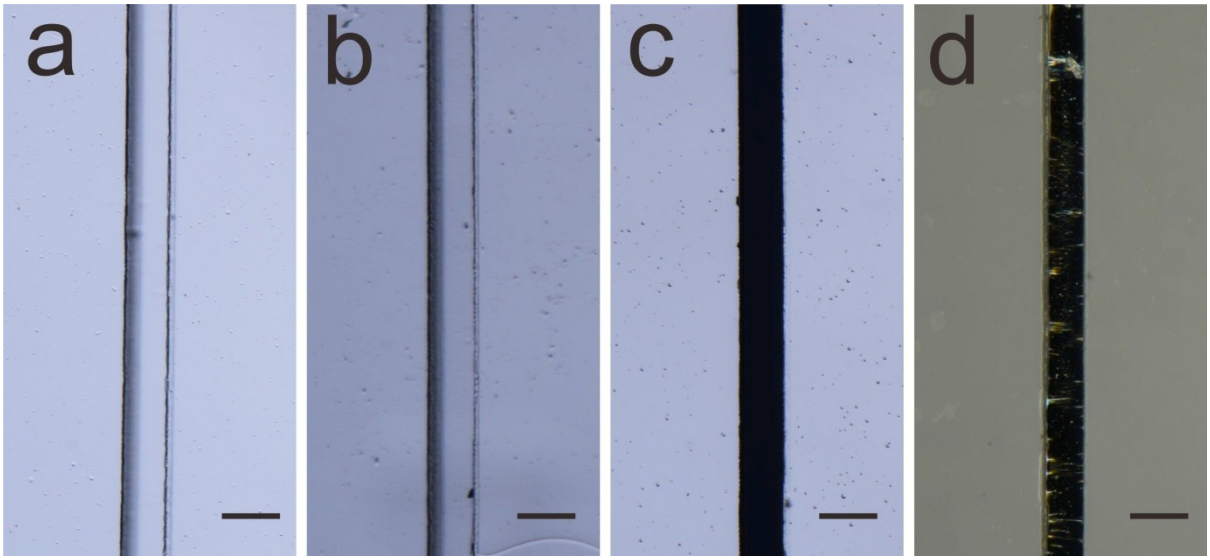

Figure S4. Microscopic images of the channel at different stages of the patterning process. a-b) PDMS channel before and after sealing with a PVA film. c) The PDMS channel filled with LM. d) The LM pattern after the PVA film is dissolved. (The scale bar is 100μm)

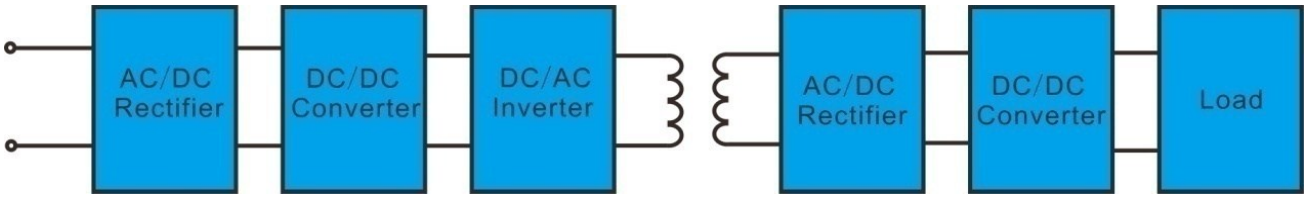

Figure S5. Scheme of a wireless charging system.

Optimization of transmission efficiency

The transmission efficiency was optimized by observing the ratio between the input (transmitted, P_{in}) and output (received, P_{out}) power at a current ranging from 100 and 1200 mA at 5 V. Figure S5a shows the variable load adaptive test of LM wireless powering, the receiver was connected to the adjustable electronic load meter, and the transmitting coil and receiving coil center alignment, the vertical distance of 2mm. As shown in Figure S5b, where the Iout increases almost linearly along with the increase of the input and output power before 700mA. Thus, the wireless power transmitter can adjusts the transmit power to provide the required power. Beyond 700 mA, the output power decline (Figure S5b), which is ascribed to high internal friction at high currents. Similarly, the power efficiency has a global maximum of 60 % at 500 mA, and stays between 40 and 60 % efficiency for

currents between 200 and 1200 mA (Figure S5c). Therefore, the LM wireless power transmitter can be employed for various electrical appliances with different current requirements.

Effect of displacement on wireless power trasnfer (WPT) efficiency

Up to this point, the charging of a battery was done at optimal conditions, meaning both the transmit and receiving coil are flat and the receiving coil was located in the center of the transmit coil at a distance of 2 mm. By displacing the receiving coil in x, y or z-direction with the aid of an x, y, z-stage, the effect of displacement on the power as well as efficiency is determined. For displacements up to 10 mm (x-axis), 15 mm (y-axis) and 10 mm (z-axis) the power efficiency is still high enough to allow efficient charging. The larger the displacement from the center point is the lower the output power at the load is, and the corresponding efficiency is low due to weakening of the electromagnetic field. The short-range efficient power transfer is typical for short distance inductive wireless power transfer, as the electromagnetic field is weakening with the square of the distance.

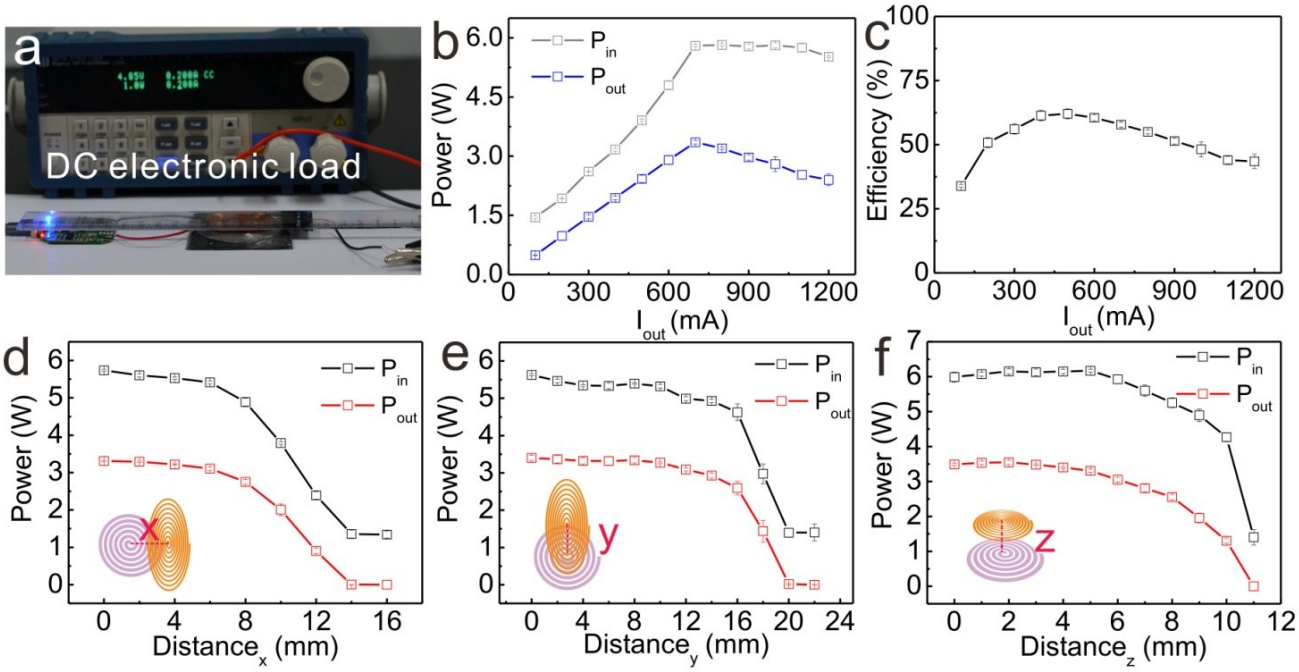

Figure S6. a) Digital image of loaded test of the LM wireless powering. b-c) Dependence of the input (transmitted, P_{in}) and output (received, P_{out}) power on variation of current employed at the load. The efficiency is also indicated. d-f) Change of output power (P_{out}) at the load and

employed input power (P_{in}) at the transmit coil upon displacement of the receiving coil along the x-axis (d), y-axis (e), and z-axis (f)

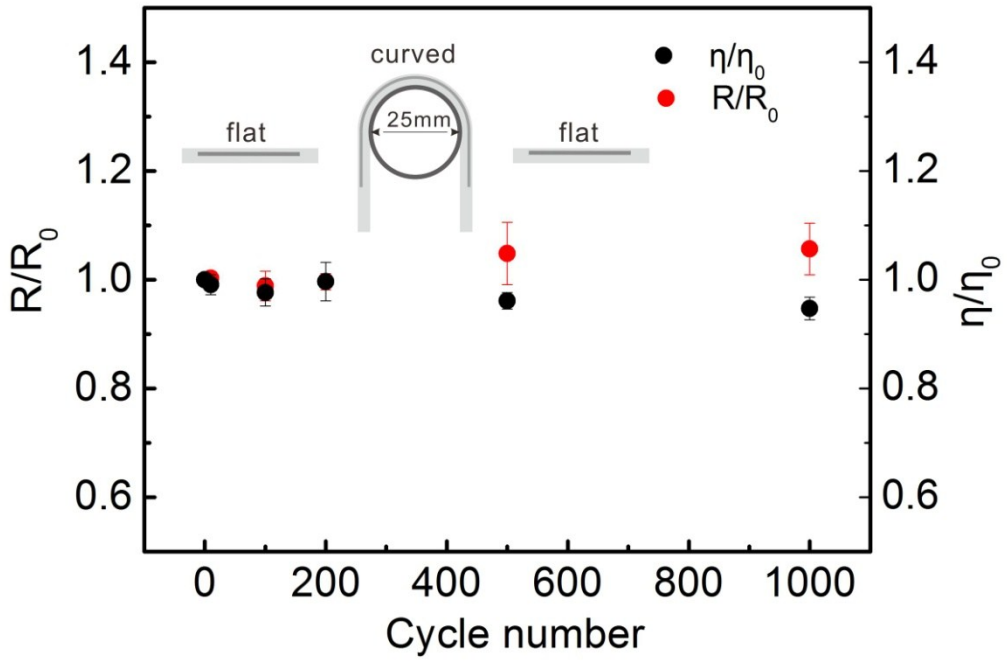

Figure S7. Fatigue test of a LM based transmit coil (LM line width 1000 μm) fabricated by the sacrificial sealing method. The diagram shows the dependence of normalized resistance (R/R_0) and normalized WPT efficiency (η/η_0) of the coil on number of bending cycles (bending diameter 25 mm).

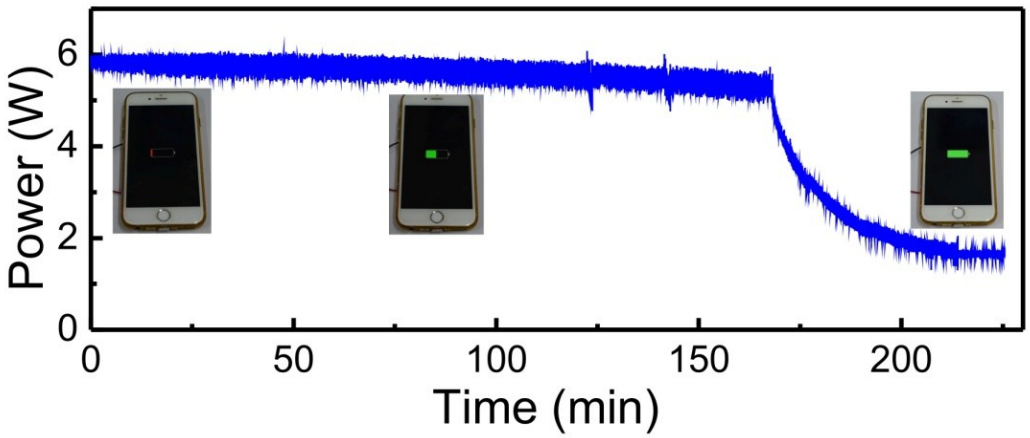

Figure S8. The real-time imput power of the transmitter during charging of a mobile phone.

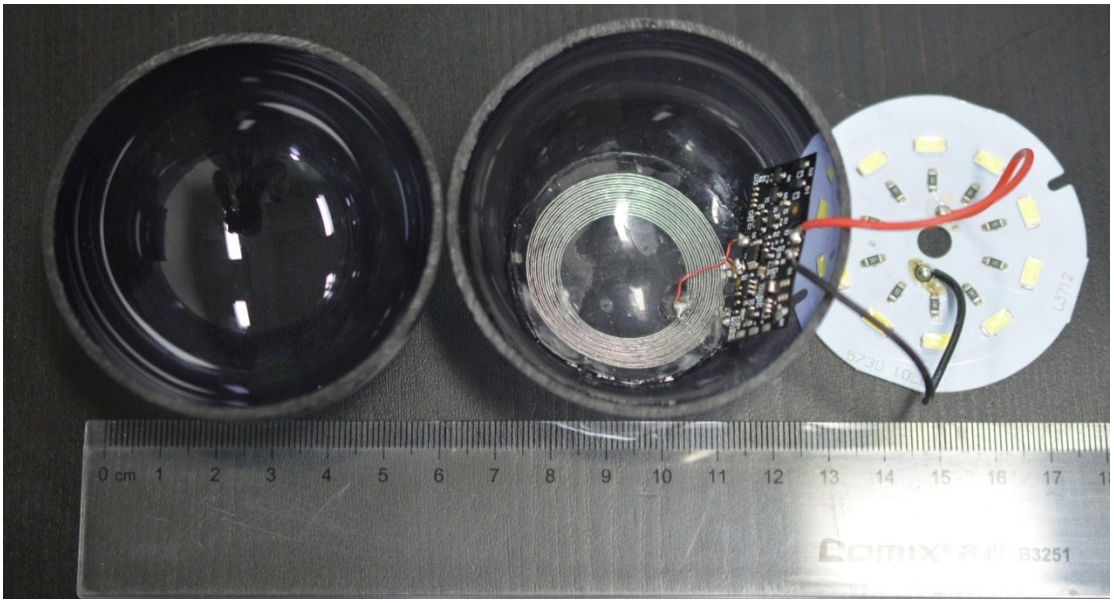

Figure S9. Digital image shows the spherical light bulb interior, where flexible receiving coil is able to adapt to the curvature of the bulb.

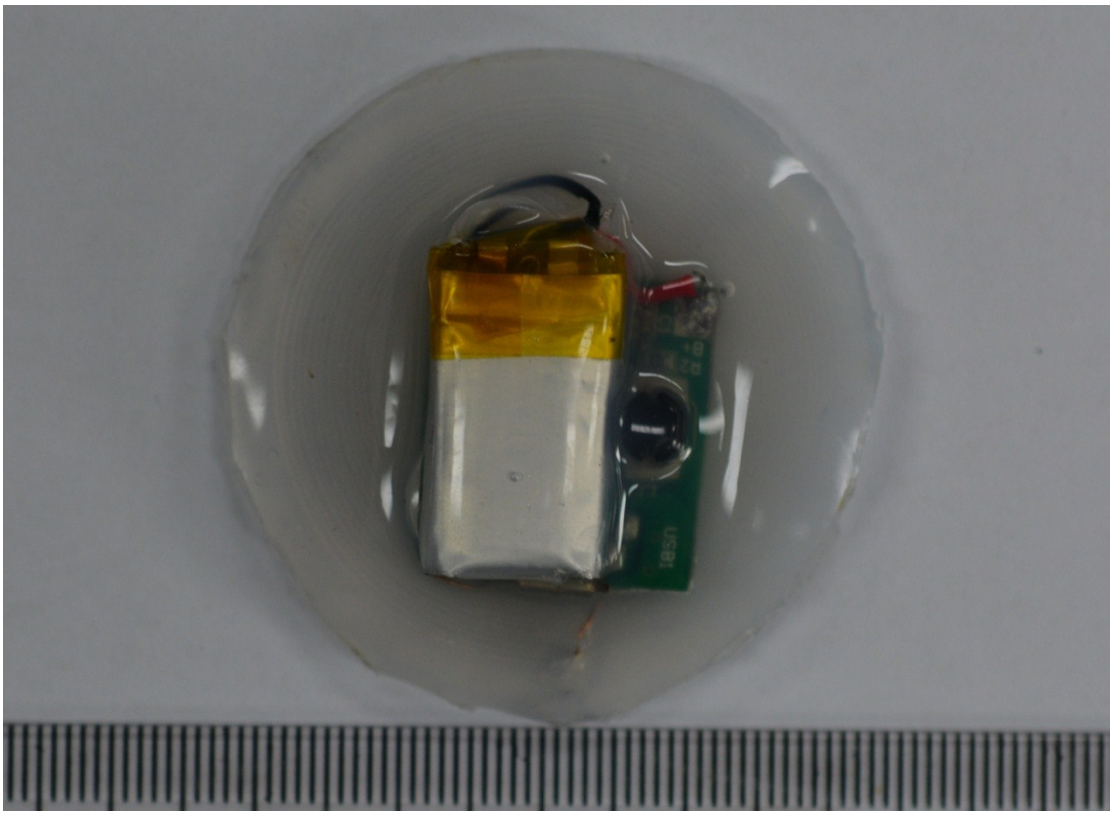

Figure S10. Digital image of the employed implantable device.

Figure S11. Digital image of a bluetooth hat equipped with a wireless receiver.